ORIGINAL PAPER

Effects of topography on status and changes in land-cover patterns, Chongqing City, China

**Yi Zhao · Mizuki Tomita · Keitarou Hara ·
Michiro Fujihara · YongChuan Yang ·
LiangJun Da**

Abstract Chongqing Municipality, located on the upper reaches of the Yangtze River, is one of China's four largest megacities, comparable with Shanghai, Beijing, and Tianjin. In recent years, Chongqing and its surroundings have been experiencing severe environmental problems, such as urbanization, pollution, and deforestation, due to the rapid economic development of China's inland region. Understanding the current land-cover status over a wide scale, as well as changes in land-cover over time, are necessary for improving the urban environment and implementing conservation measures in the Chongqing region. In this study, remote-sensing data from 1993 and 2001 were used to analyze land-cover changes. Due to the distinctive mountainous topography of Chongqing, digital topography data shuttle radar topography mission (SRTM)-3 were also used. The results of the analysis showed that urban area increased from 109.91 km^2 (5.7%) in 1993 to 166.84 km^2 (8.7%) in 2001. This increase came at the expense of agricultural and vegetated areas. Although irrigated paddy field and dry farm land decreased due to the development, these two land-cover categories still covered the largest agricultural area. Correlating the land-cover changes with different topography types, the results showed that forest covered a larger area and enjoyed a higher frequency of distribution at higher elevations and on steeper slopes. The increase in urban area, in contrast, was apparently associated with lower elevations and milder slopes. These results indicate that incorporating terrain characteristics into remote-sensing analysis can be a useful tool in developing conservation measures for vegetated and agricultural areas.

Y. Zhao (✉)
Graduate School of Informatics, Tokyo University of Information
Sciences, 4-1 Onaridai, Wakaba-ku, Chiba 265-8501, Japan
e-mail: zhaoyisoul@gmail.com

M. Tomita · K. Hara
Department of Environmental Information,
Faculty of Informatics, Tokyo University of Information
Sciences, Chiba, Japan

M. Fujihara
Awaji Landscape Planning and Horticulture Academy/Institute
of Natural and Environmental Sciences, University of Hyogo,
Hyogo, Japan

Y. Yang
Key Lab of Three Gorges Reservoir Region's Eco-Environment,
Ministry of Education, Chongqing/Faculty of Urban
Construction and Environmental Engineering, Chongqing
University, Chongqing, China

L. Da
Department of Environmental Sciences, East China Normal
University, Shanghai, China

Introduction

Rural landscapes surrounding urban areas provide ecological, economic, and cultural services for humans and wildlife (Wasilewski and Krukowski 2004). Conversion of rural land cover into nonrural land, however, has became a serious problem in many countries (Haryriye 2007). Recently, the effects of urbanization on agricultural areas, forests, other natural areas, and watersheds have received increasing international attention (Antrop 2000; Gautam et al. 2003; Haryriye 2007; Lopez et al. 2001; Hatt et al. 2004; Ojala and Louekari 2002). As part of a national policy stressing reformation and opening, China has been experiencing an unprecedented acceleration in urban

expansion since the 1980s (Long et al. 2007). Chongqing, the fourth-largest megacity in China, has been subject to especially fast economic development as the nucleus of an economic program designed to rejuvenate the inland region. This development has been accompanied by intense urbanization that is now reaching from the urban center out into the surrounding rural areas. Grübler (1994) indicates that land-cover change to urban areas usually only accounts for a small proportion compared with those of other land-cover types in most regions. The ecological impact of changes to urban area on the environment surrounding the city, however, is often more severe than that resulting from changes to other land-cover classes (Folke et al. 1997; Heilig 1994; Lambin et al. 2001). A better understanding of the characteristics and recent changes in Chongqing's land cover will thus provide useful insights that will facilitate decision-making in establishing conservation measures and urban planning. Chongqing is called the Mountain City due to its distinctive surrounding mountainous terrain. As most of its urban area is distributed on flat land, the land-cover patterns depend heavily on the surrounding undulating landforms. Topography is usually regarded as a major factor influencing human activity, which in turn affects land-cover and landscape patterns (Johnson and Patil 2006; Ispikoudis et al. 1993). Although some studies (Wu et al. 2006; Li et al. 2008) investigated the relationships between land cover and topography, the nature of these relationships still needs to be clarified.

Remote sensing (RS) and geographic information systems (GIS) are recognized as powerful and effective tools and are widely applied in detecting spatiotemporal dynamics of land cover (Fazal 2000; Weng 2002; Liu et al. 2003; Nagendra and Munroe 2004). In this study, these tools were used to clarify the land-cover status in Chongqing and the changes that have occurred during the recent period of accelerated urbanization. The general objectives of the study were to: (1) implement land-cover classification based on Landsat TM for 1993 and ETM+ for 2001, and (2) quantify the land-cover changes in relation to topographical factors such as elevation, slope, and aspect.

Methods

Study area

Chongqing (28°10′–32°13′N, 105°11′–110°11′E) is located in southwest China (Fig. 1) in the fold zone of the Eurasian tectonic plate. The region is part of a sensitive ecological area in the Three Gorges and is essential for conservation of ecosystems in the upper reaches of the Yangtze River (Fu et al. 2001). The city's climate is subtropical monsoon, with an annual mean temperature of 18.9°C (Chongqing Municipal Bureau of Statistics 2006). The core urban area is 5,479.3 km^2, which accounts for only 6.6% of the total municipality area. Population of the municipality is 5.67 million ans is concentrated in the core urban area. The topography surrounding the urban core is montane and hills. The highest point is 950 m on Mt. Jinyun, whereas the low-lying areas along the Yangtze River are <200 m (Fig. 2). The city is situated where the Jialing River passes through the Sichuan Basin to join into the main branch of the Yangtze, forming a peninsular.

Most forests are distributed on the mountains that surround the city, such as Jinyun, Tongluo, and Zhongliang. These are part of the Huayin Mountains and are covered by evergreen broad-leaved and conifer forest. Secondary forest is also a main forest type distributed on the mountains. The study area (1,924.02 km^2), shown as the meshed area in (Fig. 1), include the central part of the city and surrounding hills and mountains up to the peak of Mt. Jinyun. Administratively, this area comprised nine districts (Yubei, Jiangbei, Yuzhong, Nanan, Jiulongpo, Dadukou, Shapingba, and Beibei) and one prefecture (Bishan).

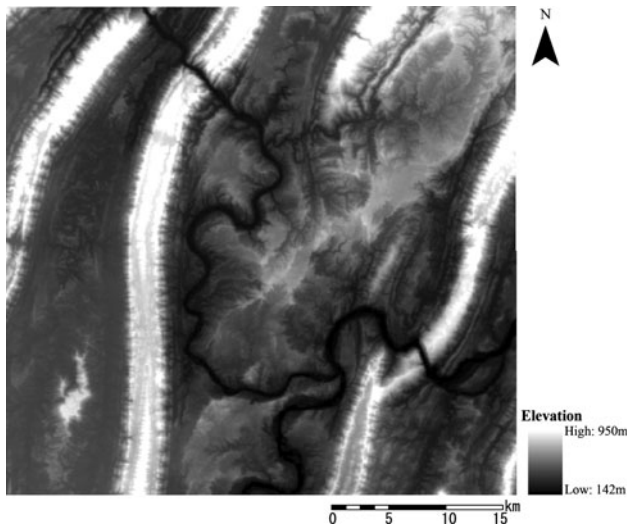**Fig. 1** Location of Chongqing, China, and study area (*meshed square*)
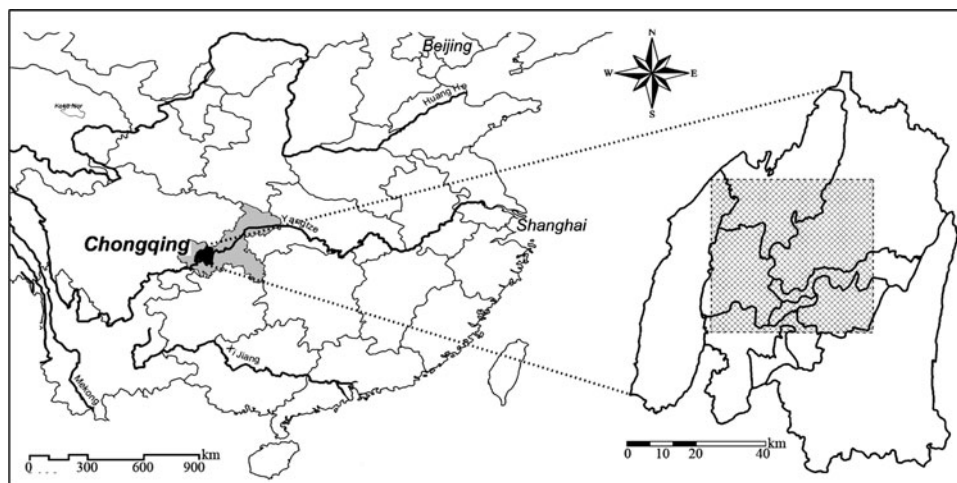
Fig. 2 Topographic data of Chongqing using 90-m shuttle radar topography mission (SRTM-3)

Reference data collection

There were 1,691 photographs taken in August 2006 and 2007 using a digital camera (D200, Nikon Corporation) with GPSMAP 60CS global positioning system (GPS) (Garmin, Ltd) to establish ground truth; 331 with GPS location were used as reference data for classification and accuracy assessment. A 10-m resolution advanced land-observing satellite (ALOS) image obtained on 20 May 2006, and aerial photographs of Chongqing central city (Chongqing Geography Information Center 2007) were also used as reference data.

Land-cover classification

The research employed Landsat TM (24 May 1993; path 128, row 39) and Landsat ETM+ (22 May 2001; path 128, row 39) data downloaded from the global land-cover facility (GLCF) of the University of Maryland, VA, USA and pregeocorrected. Bands 1–5 and 7 of the Landsat data, with 30-m spatial resolution, were used in the analysis. To avoid misclassifications, thermal infrared radiation of band 6 was removed from the analysis because of its coarse resolution (120 m for TM and 60 m for ETM+). Based on ground truth, seven classes of land cover were established: forest (Fr), dominated by natural and artificial forest, including evergreen broad-leaved and conifer trees; scrub (Sc), dominated by deciduous trees, including early succession stage woodlands and young artificial plantation; dry farm land (DFL), mostly dry fields distributed on the mountain slopes and planted with crops such as corn and wheat; irrigated paddy field (IPF), mostly distributed on the alluvial flatlands and valley bottoms; urban area (UA),

including the urban core area and arterial roads and other places covered by concrete or asphalt; barren land (BL), including sandbars, river gravels, and also construction sites where vegetation has not developed; open water (OW), consisting of rivers, lakes, and ponds.

To reduce spectral variation within a class, land-cover classification was implemented using elevation and normalized difference vegetation index (NDVI) in a hierarchical approach (Fig. 3). In the first step of analysis, Landsat TM and ETM+ images were classified into 40 classes using the unsupervised iterative self-organizing data analysis technique (ISODATA) method. These classified results were then used for separating the OW class from the other classes. In the second step, shuttle radar topography mission digital evaluation model (SRTM-3 DEM) was employed to subset the satellite data into upland (>350 m) and lowland (<350 m). This was implemented because most of the vegetated area was distributed at higher elevations. In addition, because the NDVI could partly remove the topographic effect (Saha et al. 2005; Ren et al. 2009), data was subset into vegetated and nonvegetated areas according to the threshold of NDVI through visual interpretation based on Landsat image and reference data (Ren et al. 2009). To distinguish vegetated from nonvegetated areas, the original value of NDVI between −1 and 1 were converted into 8-bit unsigned thematic (range 0–255) data. Land-cover classification was implemented separately for each generated data. For supervised classification, 166 and 201 training areas for 1993 and 2001, respectively, were extracted from reference data. The maximum likelihood method, which is widely employed to classify data, tends to suffer from the salt-and-pepper effect inherent in pixel-based classification. To eliminate this problem, the smallest areas were removed by performing an additional clumping and cell elimination by 3×1 pixels on the initial results of the classification. For verifying the accuracy of land-cover classification, 183 sample areas independent of training areas used for classification were also extracted from reference data. Because the maximum number of pixels analyzed by the software was limited, not all of pixels included in the sample areas could be used for the assessment. To address this problem, 1,000 pixels were then randomly selected from all sample areas of each land-cover class. These analyses were performed using ERDAS IMAGINE 9.1 (Leica Geosystems GIS & Mapping, LLC).

Land-cover change

To reveal the land-cover changes in relation to the distinctive mountainous topography of Chongqing, SRTM-3 data (Fig. 2) were used to generate data for elevation, slope, and aspect. Because the SRTM system for

Fig. 3 Land-cover classification. *Veg* area mainly covered by vegetation, *Nonveg* area mainly covered by nonvegetation, *ML* maximum likelihood method
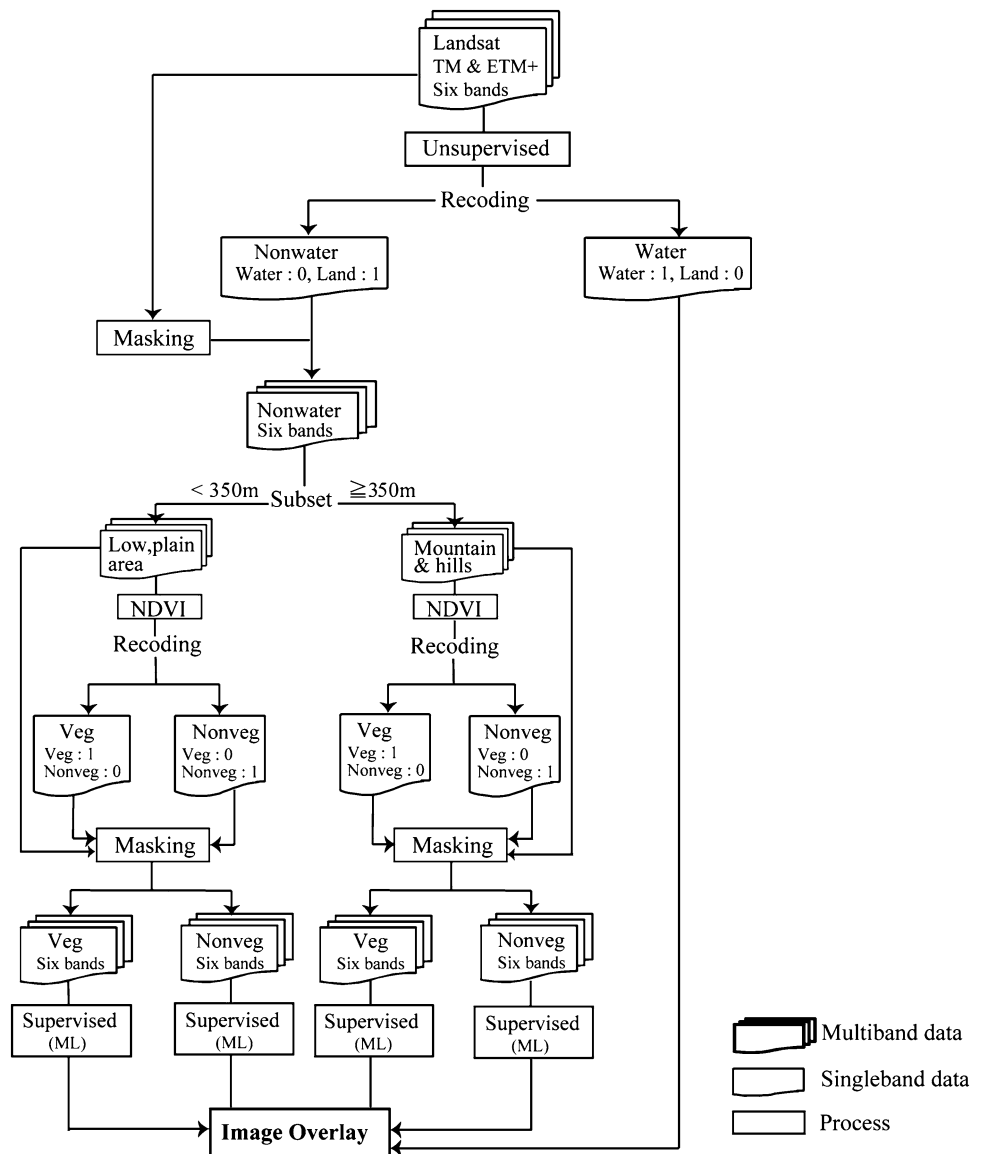
coordinating topographic data differs from that of the original Landsat data, the SRTM was rectified to a Universal Transverse Mercator (UTM) projection (WGS 84) and its minimum cell size was set as 90 m by ArcGIS 9.2 (Environmental Systems Research Institute, Inc) prior to the analysis. To select the specified area, original data in raster format was converted to polygons. In addition, elevation data created from SRTM was divided into six classes in 100-m intervals starting from an elevation of 200 m. Likewise, SRTM was also converted to slope and aspect in polygons by ArcGIS. Slope data was divided into seven classes: 0°–5°, 6°–10°, 11°–15°, 16°–20°, 21°–25°, 26°–30°, and >30°. Aspect data was divided into five classes: north (1°–45° and 316°–360°), east (46°–135°), south (136°–225°), west (226°–315°), and flatland. Based on these topography data, relative frequency distribution $\hat{p}$ of

each land-cover class and percentage of land-cover transition were used to quantify the patterns and changes in land-cover distribution. Relative frequency distribution $\hat{p}$ of land-cover classes were calculated by the following formula:

$$\hat{p} = \frac{A_{ie}}{A} \tag{1}$$

where e is the class of each elevation, slope and aspect; A_{ie} is the land-cover class i's area in the class of e; A is the total area of the study area. Transitional percentage for each land-cover class was calculated by the area converted to each of the other land-cover classes as a percentage of the total area of that land-cover class converted from 1993 to 2001. This calculation was performed for each class of elevation, slope, and aspect.

Results

Accuracy assessment

Overall accuracy of the classification was 83.4% for the 1993 image (Table 1) and 85.1% for 2001 (Table 2). Kappa statistics for the 1993 and 2001 images were 0.807 and 0.826, respectively. Although the producer's accuracy of Sc for 1993 and 2001 was only 22.1 and 25.0%, respectively, the other land-cover classes showed well-classified results. Likewise, user's accuracy of DFL in 1993 and 2001 were 54.1 and 58.0%, respectively, which were the second smallest values after Scrub. These figures showed that land-cover classes, except for Sc, were classified more accurately. The matrix of the misclassified land-cover classes also showed that >625 points in 1993 and 604 points in 2001 of Sc were misclassified into DFL.

Land-cover classification and land-cover change

Land-cover classification map showed most Fr concentrated on the outskirts of the city area (Fig. 4). Areas between the urban core and the airport and along newly constructed expressways that surround the city showed the strongest increase in UA. An increase in urbanization pressure was also be seen extending from the foothills into the outlying forest areas. Agricultural land, which includes both DFL and IPF, still covered the largest area around the city. As the results of the land-cover classification, agricultural land, DFL, and IPF decreased from 733.24 km^2 (38.2%) and 606.61 km^2 (31.6%) from 1993 to 724.09 km^2 (37.7%) and 541.25 km^2 (28.2%) in 2001 (Fig. 5), respectively. In contrast, Fr changed very little, from 303.5 km^2 (15.8%) in 1993 to 305.84 km^2 (15.9%) in 2001. In both years Fr was the third-largest cover class following IPF and DFL. Whereas agricultural land decreased, UA increased most significantly, from 109.91 km^2 (5.7%) in 1993 to 166.84 km^2 (8.7%) in 2001; Sc also increased slightly, from 90.44 km^2 (4.7%) in 1993 to 97.55 km^2 (5.1%) in 2001.

Land-cover pattern in respect to topography

Frequency distribution of land-cover classes in 1993 and 2001 showed that the study area was mainly covered by

Table 1 Accuracy assessment report of land-cover classification in 1993

Predicted	Observed							User's accuracy (%)	κ
	Fr	Sc	DFL	IPF	UA	BL	OW		
Fr	985	122	20	4	33	0	4	84.3	0.817
Sc	2	221	2	1	0	0	0	97.8	0.974
DFL	11	625	907	20	72	39	4	54.1	0.464
IPF	1	32	68	972	3	0	13	89.3	0.875
UA	0	0	0	0	888	67	3	92.7	0.915
BL	0	0	3	0	4	894	3	98.9	0.987
OW	0	0	0	3	0	0	973	99.7	0.996
Producer's accuracy (%)	98.5	22.1	90.7	97.2	88.8	89.4	97.3	$N = 7,000$	

Overall classification accuracy 83.4%; overall kappa (κ) statistics 0.807

Fr Forest, *Sc* scrub, *DFL* dry farm land, *IPF* irrigated paddy field, *UA* urban area, *BL* barren land, *OW* open water

Table 2 Accuracy assessment report of land-cover classification in 2001

Predicted	Observed							User's accuracy (%)	κ
	Fr	Sc	DFL	IPF	UA	BL	OW		
Fr	992	130	0	1	5	0	3	87.7	0.857
Sc	4	250	5	0	0	0	2	95.8	0.951
DFL	3	604	994	7	4	89	12	58.0	0.510
IPF	0	16	0	991	3	3	15	96.4	0.958
UA	0	0	1	0	980	96	20	89.3	0.876
BL	0	0	0	0	6	809	10	98.1	0.977
OW	0	0	0	1	2	3	938	99.4	0.993
Producer's accuracy (%)	99.2	25.0	99.4	99.1	98.0	80.9	93.8	$N = 7,000$	

Overall classification accuracy 85.1%; overall kappa (κ) statistics 0.826

Fig. 4 Land-cover classification map in 1993 and 2001. Land-cover classes are defined in Table 1
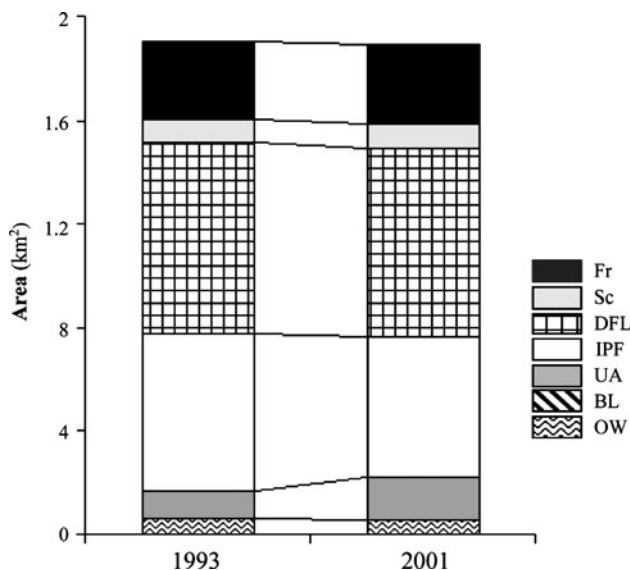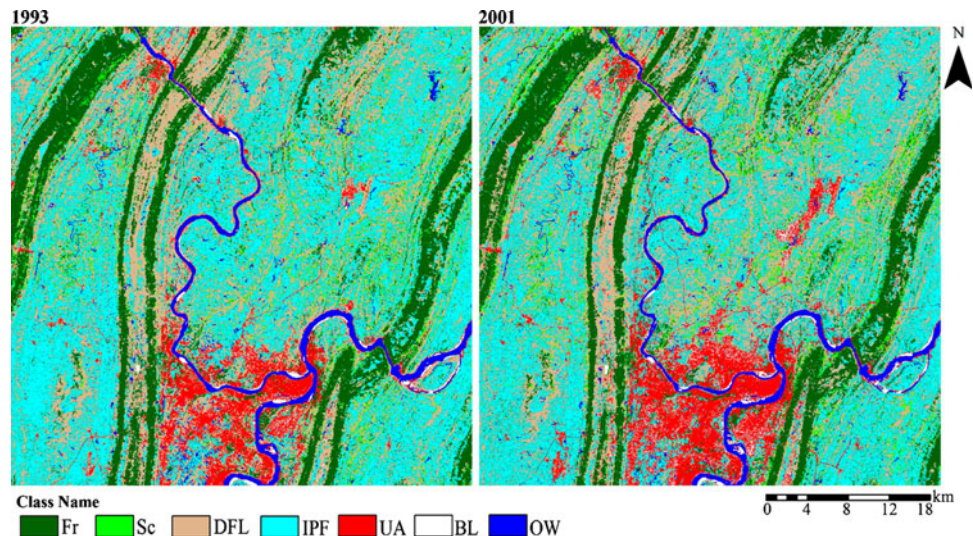

Fig. 5 Land-cover classification proportion for each land cover. Land-cover classes are defined in Table 1

<10° were mainly covered by IPF and DFL (Fig. 6b). Frequency distribution of all land-cover classes decreased as the slope became steeper, although Fr showed a slighter change than the other classes. More than 90% of the area of all land-cover classes except for Fr and Sc were distributed <15°. UA was mainly distributed on gentle slopes <5° and showed the highest frequency next to DFL and IPF for this slope range. UA also showed a constant increasing rate for all slopes. DFL combined with IPF showed the highest frequency distribution in the area <10° but decreased as the slope became steeper. Frequency distribution of each land-cover class by aspect for both 1993 and 2001showed that DFL and IPF had the highest frequency regardless of aspect (Fig. 6c). Aspect, however, mainly affects plant growth due to varying amounts of sunshine and water and thus has little effect on land-cover classes such as UA. UA thus showed a constant distribution pattern, increasing on all aspects. Fr showed the highest frequency distribution in the western aspect, where environmental factors may facilitate vegetation growth.

Land-cover change in relation to topography

Percentage of loss at each elevation showed that the rate of Fr and Sc converted to DFL was highest between 201 and 500 m, indicating that the greatest deforestation took place in these areas (Table 3). This trend was highest for 201–300 m, with the rate of Fr converted to IPF and UA 6.7% (7.6 km^2) and 5.8% (6.62 km^2), respectively. In the range of 501–600 m, Fr transitioned to DFL at a higher rate—8.2% (9.26 km^2)—than to any of the other classes. The highest rate of transition from DFL and IPF to UA—6.8% (27.06 km^2) and 3.3% (10.82 km^2), respectively—occurred between 201 and 300 m. DFL also converted obviously to Sc in the 201–500-m range, and the rate of

UA, IPF, and DFL <300 m (Fig. 6a) but that UA, IPF, and DFL decreased with elevation. In contrast, Fr increases with elevation except for the area >600 m and became a major land-cover class >400 m. These results show that less Fr is found in the foothills and lowlands due to the higher intensity of UA development. Based on field observations, artificial Fr was mainly distributed between 400 and 500 m, whereas natural Fr was distributed patchily >500 m. The results also showed that although Fr and DFL changed only slightly between 1993 and 2001, Sc increased <400 m but decreased >400 m. UA increased most drastically among all the land-cover classes. This increase became even greater as elevation rose.
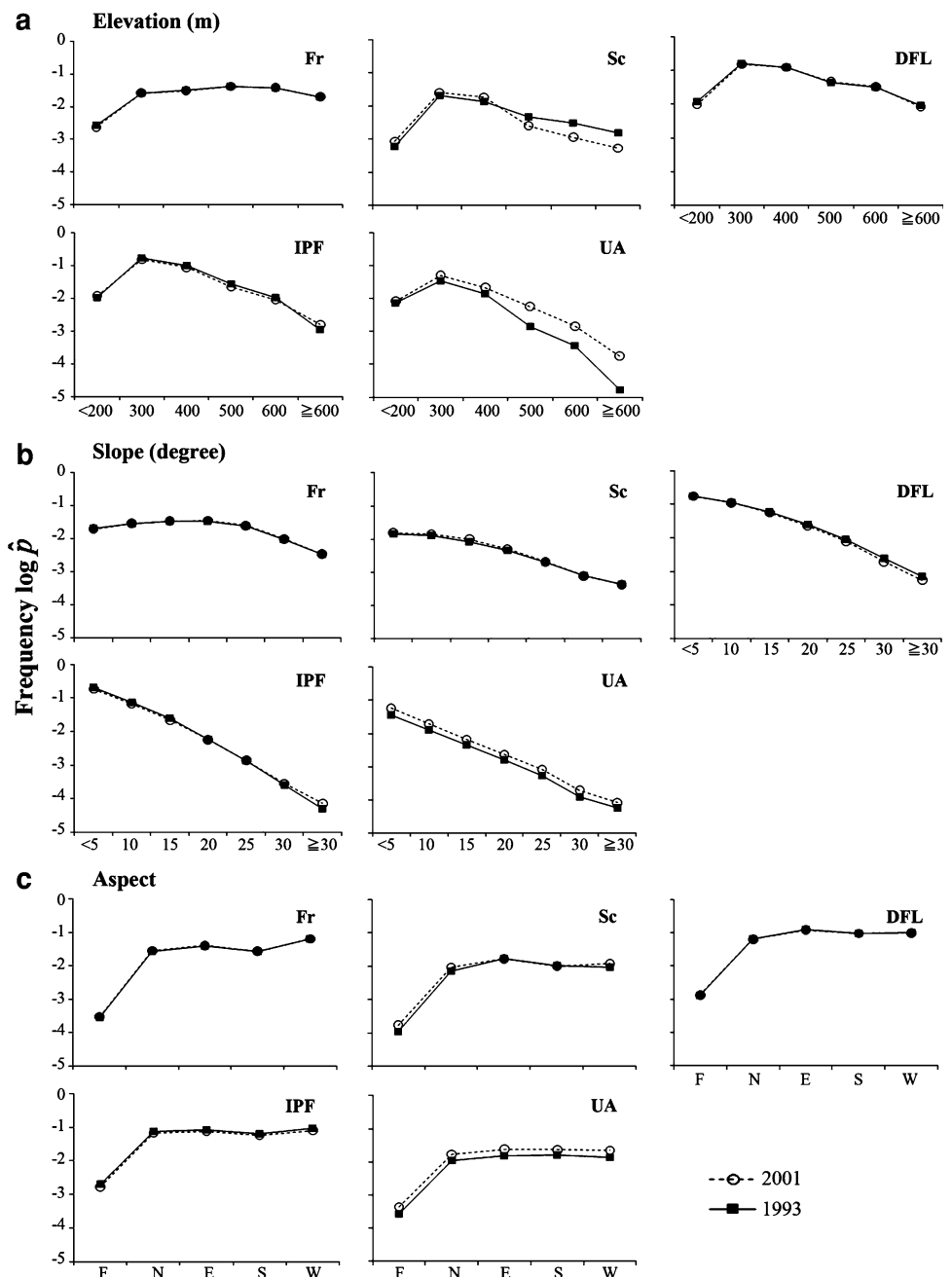
The result of frequency distribution for land cover and its changes in relation to slope classes showed that the areas

Fig. 6 Frequency distributions of land-cover classes as related to topographic conditions. *F* flat, *N* north, *E* east, *S* south, *W* west. Land-cover classes are defined in Table 1

transition from IPF to Fr and Sc—3.9% (12.71 km^2) and 3.2% (10.32 km^2), respectively—occurred in the 201-300-m elevation range.

Loss of Fr and Sc to DFL for slopes <5° was 12.2% (13.59 km^2) and 24.0% (22.33 km^2), 14.9% (16.6 km^2) and 22.6% (21.0 km^2) at 6°–10°, 12.2% (13.51 km^2) and 13.1% (12.13 km^2) at 11°–15°, respectively (Table 4). These figures showed the greatest loss <15° of Fr and indicate a high rate of deforestation at these slopes. Percentage loss of DFL to UA was highest—9.7% (34.64 km^2)—for <5°; and the highest rate of transition from Fr to IPF and UA was <10°.

Percentage of loss of Fr to DFL, IPF, and UA was highest for the western aspect at 17.3% (17.4 km^2), 7.1% (7.16 km^2) and 4.6% (4.63 km^2), respectively (Table 5). This result shows that western aspect areas are heavily influenced by urban development, deforestation, and reclamation. On the other hand, DFL and IPF converted to Fr in the west were 5.7% (19.82 km^2) and 3.8% (10.93 km^2), respectively, and to Sc in the east were 5.7% (19.78 km^2) and 1.7% (5.01 km^2), respectively. The highest rate of transition for DFL and IPF in both east and west was to UA, at 5.2% (18.36 km^2) and 2.3% (6.65 km^2), respectively.

Table 3 Transitional percentage of land-cover classes by elevation

Land-cover classes	Total area of loss (km^2)	Converted types	Percentage (%) of loss on each elevation (m)					
			≦200	300	400	500	600	>600
Forest	113.26	Scrub	0.4	5.9	4.6	5.9	1.3	0.5
		Dry farm land	0.8	9.2	11.5	19.4	8.2	2.9
		Irrigated paddy field	1.2	6.7	3.5	4.7	0.8	0.4
		Urban area	1.2	5.8	1.4	1.8	0.3	0.1
Scrub	98.0	Forest	0.2	3.5	3.4	6.1	3.7	2.3
		Dry farm land	0.8	25.3	17.6	23.1	2.6	0.6
		Irrigated paddy field	0.2	5.2	1.7	1.8	0.0	0.0
		Urban area	0.0	0.8	0.3	0.4	0.0	0.0
Dry farm land	399.28	Forest	0.4	3.6	3.3	5.7	2.0	0.9
		Scrub	0.2	6.4	5.4	5.9	0.1	0.0
		Urban area	0.7	6.8	3.5	4.9	0.5	0.1
Irrigated paddy field	325.92	Forest	0.5	3.9	1.8	2.2	0.3	0.1
		Scrub	0.1	3.2	1.7	1.9	0.0	0.0
		Urban area	0.3	3.3	1.8	2.5	0.1	0.0

Table 4 Transitional percentage of land-cover classes by slope

Land-cover classes	Total area of loss (km^2)	Converted types	Percentage (%) of loss on each slope (°)					
			≦5	10	15	20	25	30	>30
Forest	111.08	Scrub	3.2	4.5	4.3	2.9	1.7	0.9	0.5
		Dry farm land	12.2	14.9	12.2	7.6	3.6	1.1	0.4
		Irrigated paddy field	6.2	5.4	3.3	1.5	0.6	0.1	0.0
		Urban area	4.5	3.3	1.9	1.0	0.5	0.1	0.0
Scrub	92.95	Forest	3.0	4.6	4.8	4.3	2.7	1.3	0.6
		Dry farm land	24.0	22.6	13.1	5.5	2.0	0.4	0.2
		Irrigated paddy field	4.5	2.9	1.2	0.4	0.1	0.0	0.0
		Urban area	0.8	0.5	0.2	0.0	0.0	0.0	0.0
Dry farm land	358.31	Forest	3.6	4.8	4.3	3.0	1.5	0.6	0.2
		Scrub	5.2	5.6	3.9	1.8	0.7	0.1	0.0
		Urban area	9.7	4.4	1.6	0.5	0.2	0.0	0.0
Irrigated paddy field	280.15	Forest	3.7	3.1	1.9	0.8	0.3	0.1	0.0
		Scrub	3.5	2.1	1.0	0.3	0.1	0.0	0.0
		Urban area	5.7	1.6	0.4	0.1	0.0	0.0	0.0

Discussion

In this study, land-cover status and change in and around Chongqing city were quantified using Landsat TM (1993) and Landsat ETM+ (2001) image data, along with SRTM-3 topographic data. The results showed that this combination of topographic and remote-sensing imagery is a useful tool for clarifying land-cover distribution patterns and changes. As the result of the accuracy assessment for land-cover classification, most land-cover classes, including Fr, IPF, UA, BL, and OW, were classified properly (Tables 1 and 2). The spectral separability of Sc and DFL,

however, are very low and thus difficult to accurately classify. Also, overall classification accuracy for both 1993 and 2001 exceeded 80%, which also suggests this hierarchical approach is effective in reducing misclassification in an undulating area.

Analysis of land-cover change indicated that an increase in UA came at the expense of agricultural land, including both DFL and IPF. This urbanization trend was strongest between the urban core and the airport and along newly constructed expressways that surround the city. Similar situations, in which deforestation and habitat fragmentation occurs along newly built roads, have been reported for

Table 5 Transitional percentage of land-cover classes by aspect

Land-cover classes	Total area of loss (km²)	Converted types	Percentage (%) of loss on each aspect				
			Flat	North	East	South	West
Forest	100.5	Scrub	0.1	3.5	5.1	3.0	5.5
		Dry farm land	0.2	8.9	14.0	11.3	17.3
		Irrigated paddy field	0.1	3.8	3.5	3.3	7.1
		Urban area	0.1	2.4	2.2	2.4	4.6
Scrub	85.95	Forest	0.0	3.1	8.5	4.1	3.7
		Dry farm land	0.2	11.1	24.1	18.0	15.2
		Irrigated paddy field	0.0	2.1	3.1	2.0	2.5
		Urban area	0.0	0.4	0.5	0.4	0.4
Dry farm land	349.81	Forest	0.1	3.2	4.0	3.3	5.7
		Scrub	0.1	3.2	5.7	3.8	3.6
		Urban area	0.1	3.3	5.2	4.4	4.2
Irrigated paddy field	289.35	Forest	0.1	2.2	1.5	1.4	3.8
		Scrub	0.1	1.7	1.7	1.3	2.0
		Urban area	0.1	1.7	2.2	2.2	2.3

other regions (Saunders et al. 2002; Bresee et al. 2004). Moreover, topography in Chongqing is considered to be one of the most important environmental factors that influence the patterns and changes in land-cover (Diao 1990). Following the undulating terrain, the city is expanding in a star shape rather than the ring shape shown by most cities located on flat land. Results of this analysis also showed that although DFL and IPF clearly decreased, they still cover the largest area and are the major land-cover type around Chongqing. The highest rate of agricultural land converted to UA occurred in the areas <300 m elevation and <10° of slope, which are most easily developed. Several studies indicated that abandonment of marginal agricultural land can produce indirect environmental benefits, such as forest regeneration (Huston 2005; Falcucci et al. 2007), but agricultural land is representative of the Chongqing regional landscape, and a drastic reduction may result in disturbance of the regional ecosystem and an increased threat to diverse species that depend on agricultural habitats.

Fr, which is the second largest land-cover class after agricultural land, was found to have not decreased significantly during the 8 years of this study period. In addition, an increase in Sc was recorded. This may be due to the recent "grain-for-green" policy, in which agricultural land is allowed to revert to forest (Long et al. 2008), and also to vegetation regeneration on abandoned farmland. The results using topographic data also showed that the greatest amount of Fr was concentrated on the mountains surrounding the city. Fr distribution increased at higher elevations and steeper slopes. Stretches of Fr patch concentrated in the mountains form continuous habitat corridors, which can be expected to play an important role in conserving biodiversity in the study area (Forman and Godron 1986; Horskins et al.

2006). On the other hand, some Fr and Sc land was converted to agricultural land at lower elevations and gentler slopes, where vegetated areas are heavily influenced by urban development and reclamation. A high transitional rate of Fr and Sc to DFL was also recorded on steep slopes of 16°–20°, indicating that expanding urbanization is not limited to the flat areas but that reclamation and logging have increased on the steeper slopes as well. The highest frequency distribution of Fr was recorded for the western aspect, but most of the other classes showed less difference according to aspect. This may be due to an increase in newly planted trees in the western aspect or to shadows from the surrounding hills that resulted in some misclassification.

UA was the only land-cover class that increased, indicating that urbanization may be the cause of decreased agricultural land and deforestation. Urbanization can also be a main causal factor in ecosystem degradation and heat-island phenomenon (Orville et al. 2000; Grove and Burch 1997; Pickett et al. 2001). In particular, our field survey and analysis results confirmed that increased urbanization was not limited to the low, flat areas. A large number of residential and amusement facilities also increased at higher elevations near the forested areas. Also, as the highly urbanized area gradually expands from the urban core into the surrounding agricultural land, it can decrease the effectiveness of the rural landscape as a buffer zone between Fr and UA, leading to increases in ecological impacts such as diversity loss, deforestation, and fragmentation (Baker 1989, 1992; Hansen and Rotella 2001; Hansen et al. 2004; DeFries et al. 2005). Furthermore, as the UA expands outward, land reclamation and logging activities may be pushed higher up into the mountains, again leading to increased ecological impacts on the forests that thrive at these higher elevations and steeper slopes.

Based on our results, effective conservation measures for protecting agricultural land and forests from urbanization due to the recent rapid economic development are urgently required. Reclamation and deforestation on the slopes is becoming an especially important issue. These measures will require more refined base information for environmental management and planning, including more accurate land-cover classification maps. Moreover, the Chongqing region serves as an sensitive ecological ecotone between the lower and upper reaches of the Yangtze River (Fu et al. 2001) and is thus very important for maintaining ecosystem quality in the inland region. Regional conservation will require continued monitoring of land-cover changes and evaluation of environmental effects, coupled with not only more detailed resolution topography data but also with social and economic data.

References

Antrop M (2000) Changing patterns in the urbanized country-side of Western Europe. Landsc Ecol 15:257–270

Baker WL (1989) Landscape ecology and nature reserve design in the boundary water canoe area, Minnesota. Ecology 70:23–35

Baker WL (1992) The landscape ecology of large disturbances in the design and management of nature reserves. Landsc Ecol 7:181–194

Bresee MK, Moine JL, Mather S, Brosofske KD (2004) Disturbance and landscape dynamics in the Chequamegon National Forest Wisconsin USA, from 1972 to 2001. Landsc Ecol 19:291–309

Chongqing Municipal Bureau of Statistics (2006) Chongqing statistical yearbook. China Statistics Press, Beijing (in Chinese and English)

Chongqing Geography Information Center (2007) Image map of Chongqing. Xi'an cartography Press, Xi'an (in Chinese)

DeFries R, Hansen A, Newton AC, Hansen MC (2005) Increasing isolation of protected areas in tropical forests over the past twenty years. Ecol Appl 15:19–26

Diao CT (1990) The geomophological environment and urban expanding in Chongqing. J Southwest China Normal Univ (Nat Sci) 15(4):484–489 (in Chinese with English abstract)

Falcucci A, Maiorano L, Boitani L (2007) Changes in land-use/land-cover patterns in Italy and their implications for biodiversity conservation. Landsc Ecol 22:617–631

Fazal S (2000) Urban expansion and loss of agricultural land—a GIS based study of Saharanpur City, India. Environ Urban 12:133–149

Folke C, Jansson A, Larsson J, Costanza R (1997) Ecosystem appropriation by cities. Ambio 26:167–172

Forman RTT, Godron M (1986) Landscape ecology. Wiley, New York

Fu BJ, Liu GH, Chen DL, Ma KM, Li JR (2001) Scheme of ecological regionalization in China. ACTA Ecol Sin 21:1–6 (in Chinese with English abstract)

Gautam AP, Webb EL, Shivakoti GP, Zoebisch MA (2003) Land use dynamics and landscape change pattern in a mountain watershed in Nepal. Agric Ecosyst Environ 99:83–96

Grove JM, Burch WR (1997) A social ecology approach and applications of urban ecosystem and landscape analyses: a case study of Baltimore, Maryland. Urban Ecosyst 1:259–275

Grübler A (1994) Changes in land use and land cover: a global perspective. In: Meyer WB, Turner BL (eds) Technology. University of Cambridge Press, Cambridge, pp 287–328

Hansen AJ, Rotella JJ (2001) Biophysical factors, land use, and species viability in and around nature reserves. Conserv Biol 16:1112–1122

Hansen AJ, DeFries R, Turner W (2004) Land use change and biodiversity: a synthesis of rates and consequences during the period of satellite imagery. In: Gutman G, Justice G (eds) Land change science: observing, monitoring and understanding trajectories of change on the earth's surface. Springer, Netherlands, pp 277–299

Haryriye E (2007) Land use trends during rapid urbanization of the city of Aydin, Turkey. Environ Manag 39:443–459

Hatt BE, Fletcher TD, Walsh SJ, Taylor SL (2004) The influence of urban density and drainage infrastructure on the concentrations and loads of pollutants in small streams. Environ Manag 34:112–124

Heilig GK (1994) Neglected dimensions of global land use change: reflections and data. Popul Dev Rev 20(4):831–859

Horskins K, Mather PB, Wilson JC (2006) Corridors and connectivity: when use and function do not equate. Landsc Ecol 21:641–655

Huston NA (2005) The three phases of land-use change: implications for biodiversity. Ecol Appl 15:1864–1878

Ispikoudis I, Lyrintzis G, Kyriakakis S (1993) Impact of human acitivities on Mediterranean landscape in Western Crete. Landsc Urban Plan 24:259–271

Johnson GD, Patil GP (2006) Landscape pattern analysis for assessing ecosystem condition. Springer, Boston

Lambin EF, Turner BI, Geist HJ (2001) The causes of land-use and land-cover change: moving beyond the myths. Glob Environ Change 11:261–269

Li ZJ, Ma YX, Li HM, Peng MC, Liu WJ (2008) Relation of land use and cover change to topography in Xishuangbanna, southwest China. J Plant Ecol 32(5):1091–1103 (in Chinese with English abstract)

Liu YS, Gao J, Yang YF (2003) A holistic approach towards assessment of severity of land degradation along the Greatwall in northern Shaanxi province, China. Environ Monit Assess 82:187–202

Long HL, Tang GP, Li XB, Heilig GK (2007) Socio-economic driving forces of land-use change in Kunshan, the Yangtze River delta economic area of China. J Environ Manag 83(3):351–364

Long HL, Wu XQ, Wang WJ, Dong GH (2008) Analysis of urban–rural land-use change during 1995–2006 and its policy dimensional driving forces in Chongqing, China. Sensors 8:681–699

Lopez E, Bocco G, Mendoza M, Duhau M (2001) Predicting land cover and land use change in the urban fringe: a case in Morelia city, Mexico. Landsc Urban Plan 55:271–285

Nagendra H, Munroe DK (2004) Landscape fragmentation and the analysis of land use/land cover change. Agric Ecosyst Environ 101:111–115

Ojala E, Louekari S (2002) The merging of human activity and nature change: temporal and spatial scales of ecological change in the Kokemäenjoki river delta, SW Finland. Landsc Urban Plan 61:83–98

Orville RE, Uffines G, Nielsen-Gammon J, Zhang R, Ely R, Steiger S, Philips S, Allen S, Read W (2000) Enhancement of cloud-to-ground lightning over Houston, Texas. Geographys Res Lett 28:2597–2600

Pickett STA, Cadenasso ML, Grove JM, Nilon CH, Pouyat RV, Zipperer Wc, Costanza R (2001) Urban ecological systems: linking terrestrial ecological, physical, and socioeconomic components of metropolitan areas. Annu Rev Ecol Syst 32:127–157

Ren GP, Zhu AX, Wang W, Xiao W, Huang Y, Li GQ, Li DP, Zhu JG (2009) A hierarchical approach coupled with coarse DEM information for improving the efficiency and accuracy of forest mapping over very rugged terrains. For Ecol Manag 258:26–34

Saha AK, Arora MK, Csaplovics E, Gupta RP (2005) Land cover classification using IRS LISS III image and DEM in a rugged terrain: a case study in Himalayas. Geocarto Int 20:33–40

Saunders SC, Mislivets MR, Chen J, Cleland DT (2002) Effects of roads on landscape structure within nested ecological units of the Northern Great Lakes region, USA. Biol Conserv 103:209–225

Wasilewski A, Krukowski K (2004) Land conversion for suburban housing: a study of urbanization around Warshaw and Olsztyn, Poland. Environ Manag 34:291–303

Weng QH (2002) Land use change analysis in the Zhujiang Delta of China using satellite remote sensing, GIS and stochastic modeling. Environ Manag 64:273–284

Wu XP, Tang ZY, Cui HT, Fang JY (2006) Land cover dynamics of different topographic conditions in Beijing. J Plant Ecol 30(2):239–251 (in Chinese with English abstract)